Available online at www.sciencedirect.com
ScienceDirect
Journal of Hazardous Materials 152 (2008) 527–535
Journal of Hazardous Materials
www.elsevier.com/locate/jhazmat

Removal of phosphate from aqueous solutions and sewage using natural and surface modified coir pith

K. Anoop Krishnan *, Ajit Haridas

Environmental Technology, Regional Research Laboratory (CSIR), Industrial Estate Post, Thiruvananthapuram 695 019, India

Received 22 December 2006; received in revised form 24 April 2007; accepted 5 July 2007
Available online 10 July 2007

Abstract

Iron impregnated coir pith (CP-Fe-I) can be effectively used for the removal of phosphate from aqueous streams and sewage. Iron impregnation on natural coir pith was carried out by drop by drop addition method. The effect of various factors such as pH, initial concentration of phosphate, contact time and adsorbent dose on phosphate adsorption was studied by batch technique. The pH at 3.0 favored the maximum adsorption of phosphate from aqueous solutions. The effect of pH on phosphate adsorption was explained by pH_{zpc}, phosphate speciation in solution and affinity of anions towards the adsorbent sites. A comparative study of the adsorption of phosphate using CP-Fe-I and CP (coir pith) was made and results show that the former one is five to six times more effective than the latter. Kinetic studies revealed that the adsorption process followed a pseudo-second order kinetic model. Adsorption followed Langmuir isotherm model. Column studies were conducted to examine the utility of the investigated adsorbent for the removal of phosphate from continuously flowing aqueous solutions.

Keywords: Adsorption; Iron impregnated coir pith; Phosphate removal; Sewage

1. Introduction

Phosphate is regarded as a major nutrient for both vegetable plants and microorganisms. But excess amount of phosphate (>1 mg/L) in effluent discharge is often responsible for eutrophication of water bodies. Recently, the sea water off coast of Thiruvananthapuram district (Kerala, India) was covered with red bloom algae which seriously affected the lives of fishermen of Kerala due to the death of tones of fishes [1]. Algal blooms causing high economic damage in coastal oceans can be caused by phosphate run-off episode [2]. In many countries, stringent regulations limit phosphorous level to 0.05 mg/L to prevent increased algae growth [3]. Phosphates input into water bodies may be from point sources and non-point sources. The point sources are well defined discharges from factories or outlets of municipal sewage streams and can be controlled using known effluent phosphate removal processes. The non-point sources include run-off from agriculture, rural and urban landscapes [4].

Various techniques have been developed for the removal of phosphate from water and wastewater [5]. Which include chemical precipitation [6,7], adsorption using suitable materials [8,9], biological treatment [10,11] and crystallization [12]. Adsorption is a good technique for the removal of trace amounts of solute from aqueous solution. Low cost and easily available materials can possibly be used as adsorbents in barriers to remove phosphate from non-point run-off. Low cost materials such as plant wastes and ordinary clays, as such, have very low adsorption capacity.

The adsorption capacity of materials can be increased by activation process or by surface modification [13,14]. The activation process enhances the pore volume and hence enlarges the diameter of the pores. During activation, the textural properties of materials may change. Two most commonly employed activation techniques are chemical activation (liquid-phase) and physical activation (gas-phase). In chemical activation process,

* Corresponding author. Tel.: +91 471 2515262; fax: +91 471 2491712.
E-mail address: sreeanoop@rediffmail.com (K.A. Krishnan).

0304-3894/$ – see front matter © 2007 Elsevier B.V. All rights reserved.
doi:10.1016/j.jhazmat.2007.07.015

carbonization and activation are carried out in a single step by the thermal decomposition of the raw material treated with certain chemicals such as H_3PO_4, NaOH, KOH, K_2CO_3 and Na_2CO_3. The physical activation involves oxidation and gasification of the material at higher temperatures. The temperatures used in chemical activation are also lower than those used in physical activation process. Therefore, the material gets a better porous structure after a chemical process [15]. Surface modification is newer technique, by which the uptake capacity of the adsorbent materials can be considerably and desirably increased [16]. Surface modification implies the functionalization of surface groups on the solid surface of the adsorbent with or with out carbonization. The newly developed functional groups may provide new sites for adsorption of solute from aqueous solutions.

Our objective was the surface modification of coir pith, a waste material of the coir industry abundantly available in places like Kerala (India), Sri Lanka and Philippines. Surface modification was carried out using Fe(III) salt solution. Batch and column adsorption techniques were employed to evaluate the adsorption process for the removal of phosphate from aqueous solutions and sewage.

2. Experimental methods

2.1. Materials

Coconut coir pith was collected from a local coir industry—Revin Coir Unit, Murukkumpuzha, Thiruvananthapuram, India. The washed and dried coir pith was used as the precursor for the preparation of the adsorbent material. All chemicals used were of analytical grade, unless otherwise mentioned. The precursor material was modified using $Fe(NO_3)_3{\cdot}9H_2O$ solution. The stock solution of phosphate was prepared by $NaH_2PO_4{\cdot}2H_2O$ in double distilled water (1000 mg/L). The experimental solution was prepared by diluting the stock solution to desired concentration using distilled water. HCl and NaOH solutions were used for pH adjustments.

2.2. Adsorbent preparation

Fresh wet coir pith was washed five times, each time with 500 mL water, followed by distilled water to remove adhered as well as soluble impurities. Then it was sun dried, slightly crushed and sieved to remove fibre particles so as to obtain coir pith (CP) for the modification process. About 50 g of CP was soaked with $Fe(NO_3)_3{\cdot}9H_2O$ solution with occasional stirring at 70 °C for 4 h. The $Fe(NO_3)_3{\cdot}9H_2O$ solution was added drop by drop in a two slot addition pattern at a rate of 15 mL/min using a peristaltic pump (Watson Marlow made, model 5058). In the first slot, 450 mL of $Fe(NO_3)_3{\cdot}9H_2O$ was added with in half an hour and for the second slot, 300 mL of the reagent was added after 1 h. Two slot additions ensured complete soaking of the material. After 4 h heating, a black, slurry type solid mass was obtained. It was dried in a hot plate at 150 °C for further half an hour followed by cooling to room temperature so as to obtain the iron(III) loaded CP (CP-Fe-I). It was washed with distilled water and filtered several times until all the physically adhered iron(III) was removed. Finally, it was dried at 70 °C for 4 h and stored in an air tight container.

2.3. Analytical methods

The adsorbent impregnated with iron was digested by the method described in the Part 3030-G of APHA [17]. The iron estimation was done by the phenanthroline method explained in the Part 3500-Fe B of APHA [17]. The FTIR spectra of CP and CP-Fe-I were recorded on Shimadzu FTIR Spectrophotometer (IR Prestige 21) using KBr pellet method. The XRD spectra of adsorbents were recorded on powder X-ray diffractometer (Philips X'pert Pro) with Cu Kα radiation employing X'celerator detector and monochromator at the diffracted beam side at 25 °C (tension: 40 kV and current: 30 mA). The variation of surface charge density, σ_0 as a function of pH at various ionic strengths of 0.01 and 0.001 M NaCl was determined using potentiometric titration method [18] employing the following equation:

$$\sigma_0 = \frac{F(C_A - C_B + [OH]^- - [H]^+)}{A} \quad (1)$$

where σ_0 is in coulomb/cm^2, A is the surface area of suspension in cm^2/L, F is the Faraday constant in coulomb/eq., C_A and C_B are the concentration of acid and alkali after each addition during titration (eq./L). $[H^+]$ and $[OH^-]$ are the equilibrium concentrations of H^+ and OH^- ions bound to the suspension surface expressed in eq./cm^2. The pH of the suspension at which σ_0 becomes zero is referred as zero point charge (pH_{zpc}). The specific surface area of the adsorbents was determined using the N_2 gas adsorption method with a Quantasorb Surface Area Analyzer, USA (Model QS-7). The phosphate content in the aqueous solution was analyzed by the ascorbic acid method described in the Part 4500-P E of APHA [17].

2.4. Adsorption experiments

The amount of phosphate ions adsorbed on the solid surface was calculated as

$$q = [(C_0 - C_A)V]/m \quad (2)$$

where q is the amount of phosphate adsorbed onto unit amount of the adsorbent (mg/g); C_o, the concentration of the phosphate ions in the initial solution (mg/L); C_A, the residual phosphate concentration in the aqueous phase after adsorption (mg/L); V, the volume of the aqueous phase (mL); and m, the weight of the adsorbent (g).

Batch adsorption experiments were conducted by agitating 0.1 g of different adsorbents such as CP and CP-Fe-I with 50 mL of $NaH_2PO_4{\cdot}2H_2O$ solution of different concentrations. The pH of the solution was adjusted using different concentrations of HCl and NaOH solutions. The solution was then subjected to constant shaking in a temperature controlled water bath shaker. At predetermined time intervals, the supernatant solution was

Table 1
Methodology of adsorption experiments

Studies conducted	Initial concentration (mg/L)	Experimental conditions			
		pH	Adsorbent dose (g/50 mL)	Agitation time (h)	Temperature (°C)
Influence of pH	50 and 100	2.0–10.0	0.1	12	30
Influence of agitation time	50	3.0	0.1	12	30
Adsorption kinetics	50–150	3.0	0.1	12	30
Adsorption Isotherm	20–200	3.0	0.1	12	30

separated by centrifugation and analyzed for residual phosphate content. The influence of pH on the adsorption of phosphate was studied by agitating 50 and 100 mg/L phosphate solutions with 0.1 g of adsorbent at different pH values (2.0–10.0) for 12 h. The kinetic study of adsorption was conducted using phosphate solution of different concentrations (50–150 mg/L) and the supernatant solution was filtered at regular intervals of predetermined time during batch adsorption process. The filtrate so obtained was analyzed for residual phosphate content. Langmuir isotherm was employed to study the adsorption equilibrium. The methodology of adsorption experiments are presented in Table 1.

2.5. Column studies

Column adsorption experiments were used to determine the effect of flow rate, inflow phosphate concentration and adsorption capacity of CP-Fe-I. Column studies are important because sewage is a continuously flowing system. Columns were designed to determine the breakthrough curve for the adsorption of phosphate from aqueous phase onto CP-Fe-I. The following experimental set up has been made for the continuous removal of phosphate from water and wastewater. A polyacrylic transparent column having 2.5 cm inner diameter and 60 cm height was used in the study. The flow diagram of the adsorption column is shown in Fig. 1. The column was uniformly filled with dried CP-Fe-I, which occasionally contained broken fibres. The inlet of the column was supported by wire gauze stacked on an adaptor to prevent the loss of adsorbent. The working volume of the column was measured as 3024 mL/day. The column worked continuously for 8 days at 30 °C.

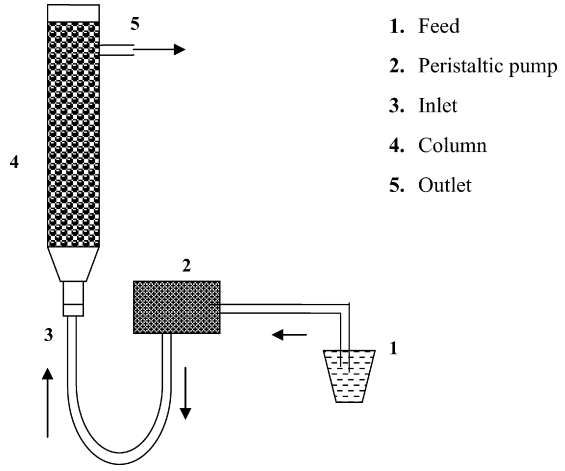

Fig. 1. Flow diagram of the adsorption column.

3. Results and discussion

3.1. Adsorbent characterization

The iron(III) content in the adsorbent was found to be 85.32 mg/g. To determine whether there is any dissolution of iron from the adsorbent during the adsorption and desorption processes, the supernatant solution was analyzed for both iron(III) and iron(II). It was observed that iron(III) was strongly bound to the adsorbent, so that it was not easily released from the adsorbent even in the presence of the alkali and alkaline earth metal cations above pH 3.0. The surface charge density as a function of pH is shown in Fig. 2. The same observations were reported by earlier workers [19,20] as well. The results clearly imply that pH influences the surface charge. The point of intersection of σ_0 against pH curves for different concentrations of electrolyte gives the pH_{zpc}. The pH_{zpc} of CP and CP-Fe-I was found to occur at 8.2 and 5.8 respectively. Based on this result, it is assumed that, adsorbent surface has been modified with iron groups. The surface area was found to be 167.4 and 155.2 m^2/g for CP and CP-Fe-I. The decrease in surface area of coir pith after impregnation indicates that the most of the adsorption sites are saturated with Fe(III) molecules which block the interaction with the N_2 molecule. Earlier workers reported the same results [21].

The FTIR spectra of CP and CP-Fe-I are shown in Figs. 3 and 4, respectively. The FTIR spectrum of CP shows

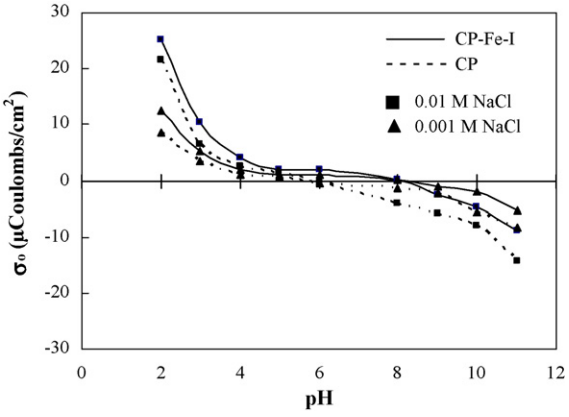

Fig. 2. Effect of pH on the surface charge density of CP and CP-Fe-I.

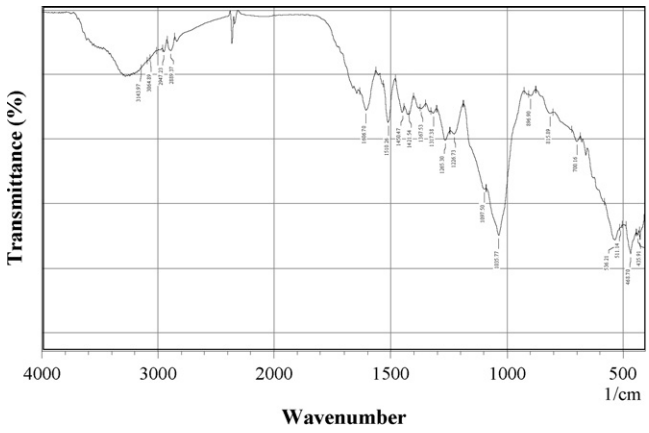

Fig. 3. FTIR spectrum of CP.

a broad absorption band around 3300 cm^{-1}, which may be attributed to the O–H group. The bands at 2947 and 2889 cm^{-1} correspond to the C–H stretching from the methylene group. The bands at 1606 and 1510 cm^{-1} reveal the aromatic C=C stretching in the phenyl ring of lignin [22]. Absorption at 1450 cm^{-1} is assigned to methoxy group of lignin in the CP [23]. In the fingerprint region (1430–910 cm^{-1}), band at 1421 cm^{-1} is attributed to O–H bending as well as C–O stretching vibration of phenol and that at 1367 cm^{-1} originates from the O–H deformation in the phenolic group. The bands at 1317, 1265 and 1035 are due to the C–O stretching vibration of primary alcohol. The band at 1097 cm^{-1} arises from the O–H bending and C–O stretching of secondary alcohol. The weak band at 896 cm^{-1} is characteristic of C–H bending vibration in β-glucosidic linkage [24].

It is very clear from the spectra that the band intensity of the carbonyl group of CP-Fe-I has diminished and shifted as compared with CP. Moreover, the number of bands in the finger print region of CP-Fe-I has decreased with respect to those in CP. In Fig. 4, bands at 1593 and 898 cm^{-1} arise from C=O stretching of hemicellulose and glucosidic linkage, respectively. The bands at 430 and 414 cm^{-1} are assigned to the stretching vibration of Fe–O in CP-Fe-I. Gong et al. [25] stated that the bands between 700 and 400 cm^{-1} are due to the Fe–O stretching vibration. The FTIR spectrum of CP-Fe-I has a new weak band at 1057 cm^{-1}

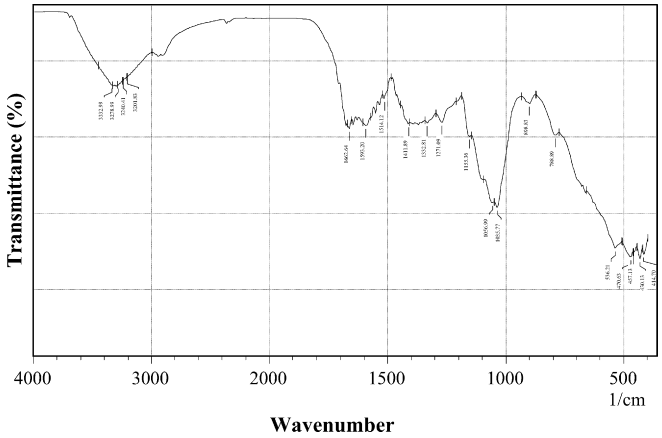

Fig. 4. FTIR spectrum of CP-Fe-I.

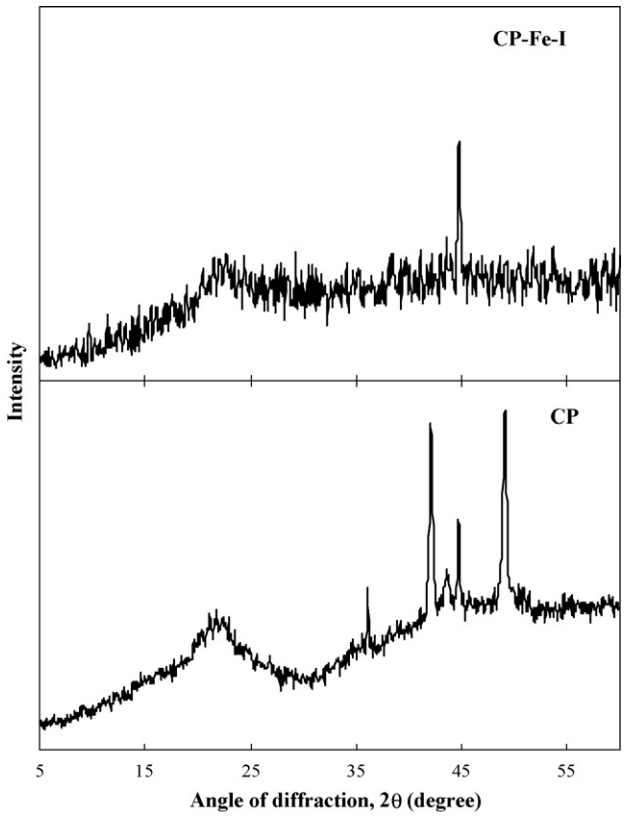

Fig. 5. XRD spectra of CP and CP-Fe-I.

for Fe–OH [26]. These observations clearly indicate the iron impregnation on CP.

The XRD spectra of CP and CP-Fe-I are shown in Fig. 5. The difference in diffraction pattern of both adsorbents may be the indication of iron impregnation in CP. The crystalline form of cellulose in CP is indicated by the scattering peak at $2\theta = 36.13$ and 42.11. The peak at 44.70 and an additional peak at 9.71 indicate the presence of iron in the CP-Fe-I. The morphology of cellulose chains in CP-Fe-I show some rearrangements due to iron impregnation, moreover the crystallanity also decreases. This is confirmed by decrease in the number and intensity of XRD peaks in CP-Fe-I. The number of peaks in 2θ range 30–50 in the XRD spectrum of CP decreased from 5 to 1 that for CP-Fe-I. This attests for the general fact that impregnation process may reduce crystallanity [27] and the structure of the CP-Fe-I is more amorphous as compared with that of CP.

3.2. Influence of pH

To examine the effect of pH on the adsorption of phosphate on CP and CP-Fe-I, batch experiments using phosphate solution with initial concentrations 50 and 100 mg/L were conducted. Investigations using 0.1 g of adsorbent in 50 mL of phosphate solution, keeping the initial solution pH values from 2.0 to 10.0, furnished the data which is presented in Fig. 6. From the figure, the effectiveness of CP-Fe-I for the quantitative removal of phosphate ions in the pH range 2.0–5.0 is quite obvious. However, CP is effective only within a narrow range of pH from 2.0

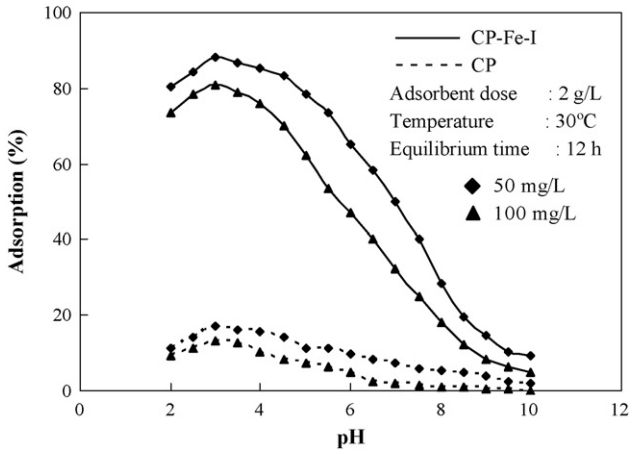

Fig. 6. Influence of pH on the adsorption of phosphate on CP and CP-Fe-I.

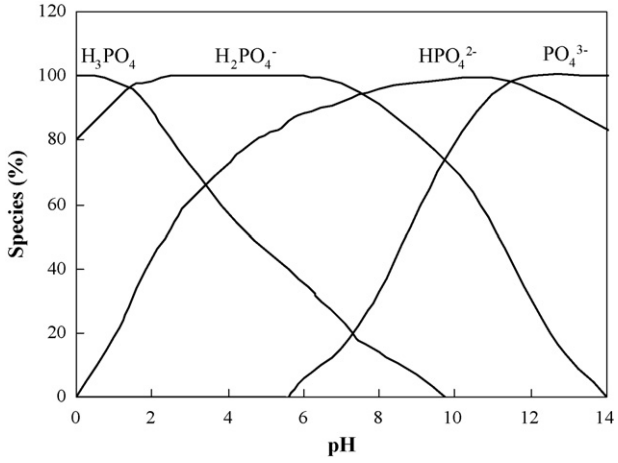

Fig. 7. Species distribution of phosphate as a function pH.

to 3.5. As the equilibrium pH increases from 2.0 to 10.0, the phosphate adsorption increases up to pH 3.0 and then decreases progressively for both the adsorbents with further increase of pH. The maximum phosphate adsorptions were 17.4% (4.35 mg/g) and 88.2% (22.05 mg/g) for CP and CP-Fe-I respectively, at pH 3.0 for an initial concentration of 50 mg/L. But at the same pH, the maximum adsorption of 13.1% (6.55 mg/g) and 81.1% (40.55 mg/g) were effected by CP and CP-Fe-I respectively from an initial concentration of 100 mg/L. The data showed that CP-Fe-I is five to six times more effective than CP for the removal of phosphate from aqueous solutions.

The pH_{zpc}, phosphate speciation in solution, affinity of anions towards the adsorbent sites, interfacial chemistry and surface chemistry are the main factors influencing the effect of pH on phosphate adsorption. Below pH_{zpc} the surface charge of the adsorbent is positive and above the surface charge is negative. The pH_{zpc} of CP-Fe-I and CP were found to be 8.2 and 5.8, below this pH, the surface charge of the adsorbents is positive. The mechanism of phosphate adsorption can be interpreted by considering the following equilibria:

$$H_3PO_4 \rightleftharpoons H_2PO_4^- + H^+, \quad p^{K_1} = 2.23 \tag{3}$$

$$H_2PO_4^- \rightleftharpoons HPO_4^{2-} + H^+, \quad p^{K_2} = 7.21 \tag{4}$$

$$HPO_4^{2-} \rightleftharpoons PO_4^{3-} + H^+, \quad p^{K_3} = 12.32 \tag{5}$$

The phosphate speciation as a function of pH is depicted in Fig. 7. The $H_2PO_4^-$ is the major species in the aqueous solution at the pH range 2.0–3.5 and is responsible for the adsorption of phosphate onto adsorbent surface. Both the adsorbents show affinity towards $H_2PO_4^-$ and the possible mechanism of ligand exchange for surface OH groups with the formation of inner sphere complex. In fact, electron transfer reactions in complexes take place through inner sphere or outer sphere mechanism. If the coordinated species of the complex is replaced, it is referred as inner sphere complex. In the case of outer sphere complex, ionizable species will be replaced. The adsorption of phosphate on CP and CP-Fe-I is described as follows:

$$CP\text{–}OH + H_2PO_4^- \xrightarrow{H^+} CP\text{–}(H_2PO_4) + H_2O \tag{6}$$

$$CP\text{–}Fe(OH) + H_2PO_4^- \xrightarrow{H^+} CP\text{–}Fe(H_2PO_4) + H_2O \tag{7}$$

At pH < 3.0, there was a gradual decrease in the adsorption of phosphate on the adsorbents under examination. This may be due to the increasing concentration of phosphoric acid, which is unable to adsorb on the solid surface. But as the pH increases, the adsorption decreases. This is because of the fact that as the solution pH increases the surface becomes more negative, creating electrostatic repulsion between phosphate ions and negatively charged surface molecules.

3.3. Influence of agitation time

Removal of phosphate by CP and CP-Fe-I with time was carried out at pH 3.0 and at a temperature of 30 °C (Fig. 8). The amount of phosphate adsorbed increased with agitation time and attained equilibrium at about 12 h for CP-Fe-I and 16 h for CP for an initial concentration of 50 mg/L. Therefore, an optimum agitation period of 12 and 16 h was selected for CP-Fe-I and CP, respectively. The curves shown in Fig. 8, present a double nature, the initial portion of the plot rises linearly and is changed

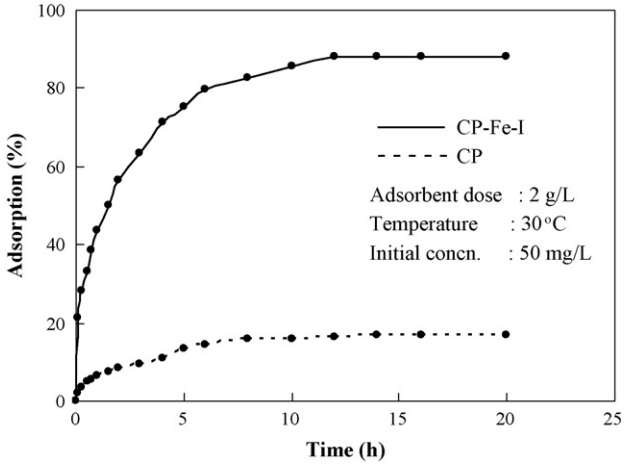

Fig. 8. Influence of agitation time on the adsorption of phosphate on CP and CP-Fe-I.

into a curve. The curves level off at 12 and 16 h of contact time for CP-Fe-I and CP respectively. After which, there is no further adsorption takes place. The rest of the adsorption studies were performed only using CP-Fe-I, since the amount of adsorption on CP was very low as compared with CP-Fe-I.

3.4. Adsorption kinetics

Kinetics of adsorption, in terms of solute uptake rate, which governs the residence time, is one of the important characteristics defining the efficiency of adsorption. The behavior of developed adsorbents was examined by studying the kinetics of phosphate removal by adsorption. The adsorption of phosphate from the liquid phase to the solid phase can be considered as a pseudo-second-order reaction. So that, the removal process taking place through the formation of inner sphere complex. The simplest way to describe the kinetics of phosphate removal, in the absence of stoichiometric data, can be represented as

$$P + M \underset{k'}{\overset{k}{\rightleftharpoons}} PM \tag{8}$$

where P is the number of active sites occupied on the adsorbent, M is the concentration of free phosphate species in solution; and PM is the concentration of phosphate bound to adsorbent. k and k' are the adsorption and desorption rate constants respectively. The rate equation for the above reaction can be represented as [28]

$$\frac{t}{q_t} = \frac{1}{kq_e^2} + \frac{t}{q_e} \tag{9}$$

where q_e and q_t are the amount of metal ion adsorbed (mg/g) at equilibrium and at time 't' respectively. The product kq_e^2 is actually the initial sorption rate represented as $h = kq_e^2$. The kinetic plots as per Eq. (9) were made for CP-Fe-I and the results for different concentrations are shown in Fig. 9. A linear straight line plot in all cases was observed with correlation coefficients of more than 0.98, and indicated that the adsorption reaction can be approximated to pseudo-second-order as suggested by Ho and McKay [28]. A similar phenomenon has been observed in the adsorption of nitrate onto various materials [29], arsenic(V) by modified calcined bauxite [30] and phosphate on dolomite [31]. The kinetic parameters k, q_e and h were calculated from the slope and intercepts of the plots and presented in Table 2. It can be noted that initial adsorption rate (h) is increased with an increase in initial phosphate concentration. The values of h increased from 25.84 to 34.17 mg/g h for CP-Fe-I with the increase of initial concentration from 50 to 150 mg/L. For the same increase in the initial concentration of phosphate, the values of k were found decrease from 4.98×10^{-2} to 0.92×10^{-2} g/mg h for CP-Fe-I. This can be due to the progressive increase in covalent interactions, relative to electrostatic interaction of the sites with lower affinity for $H_2PO_4^-$ with an increase of initial phosphate concentration. Similar observations have been reported by the earlier workers [32] who studied the adsorption characteristics of phosphate from water. The perusal of data in Table 2 reveals that for the equilibrium time, the phosphate ion adsorbed (q_e) is higher for greater values of initial phosphate ion concentration. This is obvious because more efficient utilization of the reactive sites of the adsorbent is expected due to a greater driving force by a higher concentration gradient pressure.

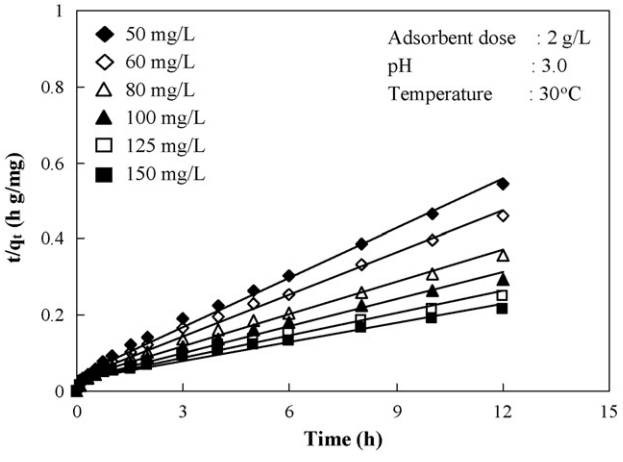

Fig. 9. Pseudo-second-order kinetic plots for the adsorption of phosphate on CP-Fe-I at different initial concentrations.

Table 2
Kinetic parameters for the adsorption of phosphate onto CP-Fe-I

Initial concentration (mg/L)	q_e-theoretical (mg/g)	k (g/mg h)	h (mg/g h)	r^2
50	22.99	4.98×10^{-2}	25.84	0.990
60	27.10	3.87×10^{-2}	28.41	0.989
80	35.46	2.45×10^{-2}	30.86	0.983
100	42.19	1.84×10^{-2}	32.70	0.979
125	51.55	1.27×10^{-2}	33.67	0.973
150	59.88	0.92×10^{-2}	34.17	0.970

3.5. Adsorption isotherm

Equilibrium studies were performed to evaluate the adsorption capacity of CP-Fe-I using different initial concentrations of phosphate ranging from 20 to 200 mg/L. The equilibrium data were analyzed using the following linearized expressions for Langmuir (Eq. (10)) and Freundlich (Eq. (11)) adsorption isotherms

$$\frac{C_e}{q_e} = \frac{1}{Q^0 b} + \frac{C_e}{Q^0} \tag{10}$$

$$\log q_e = \log K_F + \frac{1}{n} \log C_e \tag{11}$$

where q_e is the amount of solute adsorbed per unit weight of adsorbent (mg/g), C_e is the equilibrium solution phase concentration (mg/L), Q^0 and b are Langmuir constants related to the maximum adsorption capacity corresponding to complete coverage of available adsorption sites (mg/g) and energy of adsorption (L/mg) respectively. K_F and $1/n$ are the Freundlich constants related to adsorptive capacity (mg/g) and intensity of adsorption (L/mg) respectively. The values of Langmuir and Freundlich constants calculated from the linear plots of C_e/q_e versus C_e and

Table 3
Langmuir and Freundlich constants for the adsorption of phosphate onto CP-Fe-I

Langmuir				Freundlich			
Q^0 (mg/g)	b (L/mg)	r^2	Δq (%)	K_F	1/n	r^2	Δq (%)
70.92	0.10	0.988	8.74	15.44	0.31	0.926	14.12

log q_e versus log C_e, respectively at 30 °C (figure not shown) are given in Table 3. The best-fit isotherm model was selected by evaluating the correlation coefficients (r^2) and normalized standard deviation (Δq (%)). The values of Δq (%) were calculated using the following equation:

$$\Delta q\,(\%) = 100 \times \sqrt{\frac{\sum [(q_t^{\exp} - q_t^{\mathrm{cal}})/q_t^{\exp}]^2}{N-1}} \quad (12)$$

where the superscripts 'exp' and 'cal' are the experimental and calculated values and 'N' is the number of measurements. Fig. 10 typically illustrates the comparison between the calculated and observed results for the adsorption of phosphate on CP-Fe-I. The values of Δq (%) were compared to determine the appropriate type of isotherm model for phosphate adsorption. The Δq (%) value for Langmuir isotherm was much lower than that for Freundlich isotherm as shown in Table 3. Hence, the Langmuir model agrees well with these data, assuming all the adsorption sites have equal energy, while surface characterization of CP-Fe-I clearly suggests a range of site energies. Earlier studies in this direction have clearly demonstrated that the Langmuir equation gives adequate results in many cases where surface heterogeneity is known to be present [33]. Table 4 presents the comparison of adsorption capacity of CP-Fe-I with that of other adsorbents for the removal of phosphate from aqueous solutions. The comparison showed that CP-Fe-I is a good adsorbent for the adsorption of phosphate from water and wastewater. Additional research is required to test the effect of temperature on Q^0 and b for the adsorption of phosphate from aqueous solutions onto CP-Fe-I and the studies are underway.

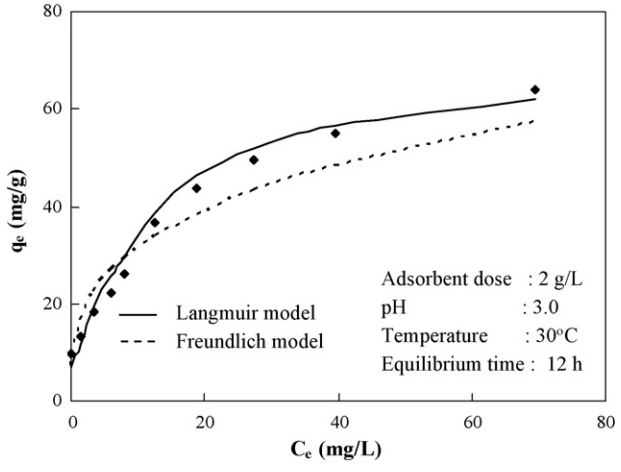

Fig. 10. Plots of q_e vs. C_e for the adsorption of phosphate on CP-Fe-I. Legends represent experimental data.

Table 4
Comparison of adsorption capacity of CP-Fe-I with other adsorbents for phosphate removal

Adsorbent	Q^0 (mg/g)	Reference
Fe(III)/Cr(III) hydroxide	6.53	[32]
Iron oxide tailing	8.21	[34]
CP-Fe-I	70.92	This work
FA	63.22	[35]
FA700	58.92	[35]
FA0.25	78.44	[35]
La/JB01	20.04	[36]
La/JB02	33.34	[36]
Cationized bark	12.06	[37]
Cationized wood	12.16	[37]

Table 5
Physico-chemical characteristics of sewage

Composition in mg/L
BOD_5: 150; COD: 281; total solids: 892; total suspended solids: 460; total nitrogen: 23; total phosphate: 9.2; oil and grease: 30.3; VSS: 390
pH: 7.6

3.6. Test with sewage

The usability of the adsorbent was tested with real domestic wastewater (sewage). Sewage was collected from local municipal stream and its characteristics are given in Table 5. Primary settled sewage was used for adsorption studies. The amount of phosphate in the sewage was low (9.2 mg/L). It was then spiked with a phosphate solution so that the final concentration of phosphate was 50 mg/L. The effect of adsorbent dose on phosphate adsorption onto CP-Fe-I from sewage is given in Table 6. The data Table 6 implies that an adsorbent dosage of 2 g/L is sufficient for the removal of 82.1% of the total phosphate from 50 mL sewage containing several other ions. It is apparent that by increasing the adsorbent dose from 1 to 6 g/L the removal efficiency increases. The complete removal of phosphate from sewage could be effected by employing 4 g adsorbent/L.

Table 6
Influence of adsorbent dose on phosphate removal from sewage

Adsorbent dose (g/L)	Removal (%)
1	69.4
2	82.1
3	91.4
4	99.8
6	99.8

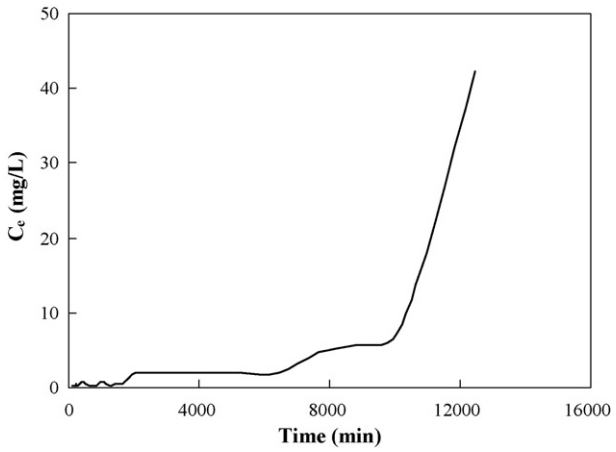

Fig. 11. Breakthrough curve for the adsorption of phosphate on CP-Fe-I.

3.7. Continuous column-mode operation

The experimental solution containing phosphate ions of initial concentration 50 mg/L was introduced into the column (upward flow method) at a fixed rate of 6.1 mL/min using peristaltic pump. Retention time was about 2.0 h. The effluent from the outlet of the column was analyzed for phosphate concentration. The adsorption column was operated for 8 days and a breakthrough curve was determined. From the breakthrough curve (Fig. 11), the adsorption capacity of CP-Fe-I was found to be 68.0 mg/g, which is in good agreement with the adsorption capacity calculated using batch adsorption technique.

4. Conclusions

Iron impregnated coir pith was found to be a suitable adsorbent for the removal of phosphate from aqueous solutions and sewage. The adsorption process is highly dependent on pH of the solution and best results were obtained at pH 3.0. The adsorption mechanism for the removal of phosphate can be described by ligand exchange reaction between the coordinated OH groups and the phosphate ($H_2PO_4^-$) ions. The iron impregnated coir pith was found to be five to six times more effective than CP for the adsorption of phosphate from aqueous solutions. A pseudo-second-order kinetic expression was used to evaluate kinetic parameters for the adsorption process. The equilibrium in the solid–solution interface was explained by Langmuir adsorption isotherm. Preliminary column adsorption experiments were conducted and the results were plotted to get the breakthrough curves. Column adsorption was found to be very effective for the removal of phosphate from aqueous solutions. Column experiments showed the adsorption capacity of CP-Fe-I was 68.0 mg PO_4/g at 50 mg PO_4/L. It appears that CP-Fe-I is better suited for low concentration run off treatment, rather than for direct removal of phosphate from point sources such as sewage outfalls.

Acknowledgements

Dr. K. Anoop Krishnan thanks the Council of Scientific and Industrial Research (CSIR), Ministry of Science and Technology, Government of India, for the financial support in the form of Research Associateship. The authors thank the Regional Research Laboratory (RRL-T), Thiruvananthapuram, India for providing laboratory facilities. The authors also thank the X-ray and Superconductivity Section of RRL-T for providing XRD spectra.

References

[1] http://www.dgukenvis.nic.in/newsletters/Newsletter13.pdf.
[2] H.D. Ruan, R.J. Gilkes, Phosphorus accumulation in farm ponds and dams in Southwestern Australia, J. Environ. Qul. 29 (6) (2000) 1875–1881.
[3] H. Behrendt, D. Opitz, M. Klein, Arch. Nat. Conserv. Landscape Res. 35 (1997) 329.
[4] G.W. Vanloon, S.J. Duffy, Environmental Chemistry, A Global Perspective, Oxford University, 2002.
[5] J.F. Duenas, J.R. Alonso, A.F. Rey, A.S. Ferrer, Characterisation of phosphorous forms in wastewater treatment plants, J. Hazard. Mater. 97 (2003) 1–3.
[6] R.G. Penetra, M.A.P. Reali, E. Foresti, J.R. Campos, Post-treatment of effluents from anaerobic reactor treating domestic sewage by dissolved-air flotation, Water Sci. Technol. 40 (1999) 137–143.
[7] L. Ruixia, G. Jinlong, T.J. Hongxiao, Adsorption of fluoride, phosphate, and arsenate ions on a new type of ion exchange fiber, J. Colloid Interface Sci. 248 (2) (2002) 268–274.
[8] A. Ugurlu, B. Salman, Phosphorus removal by fly ash, Environ. Int. 24 (8) (1998) 911–918.
[9] R. Chitrakar, S. Tezuka, A. Sonoda, K. Sakane, K. Ooi, T. Hirotsu, Selective adsorption of phosphate from seawater and wastewater by amorphous zirconium hydroxide, J. Colloid Interface Sci. 297 (2) (2006) 426–433.
[10] D. Patureau, E. Helloin, E. Rustrian, T. Bouchez, J.P. Delgenes, R. Moletta, Combined phosphate and nitrogen removal in a sequencing batch reactor using the aerobic denitrifier, *Microvirgula aerodenitrificans*, Water Res. 35 (1) (2001) 189–197.
[11] A. Gieseke, P. Arnz, R. Amann, A. Schramm, Simultaneous P and N removal in a sequencing batch biofilm reactor: insights from reactor and microscale investigations, Water Res. 36 (2) (2002) 501–509.
[12] E. Eggers, A.H. Dirkzwager, H. van der Honing, Full-scale experiences with phosphate crystallisation in a crystalactor, Water Sci. Technol. 24 (1991) 333–334.
[13] C. Namasivayam, D. Sangeetha, Equilibrium and kinetic studies of adsorption of phosphate onto $ZnCl_2$ activated coir pith carbon, J. Colloid Interface Sci. 280 (2) (2004) 359–365.
[14] T. Kasama, Y. Watanabe, H. Yamada, T. Murakami, Sorption of phosphates on Al-pillared smectites and mica at acidic to neutral pH, Appl. Clay Sci. 25 (2004) 167–177.
[15] A. Ahmadpour, D.D. Do, The preparation of active carbons from coal by chemical and physical activation, Carbon 34 (4) (1996) 471–479.
[16] A. Corma, A. Mifsud, E. Sanz, Influence of the chemical composition and textural characteristics of palygorskite on the acid leaching of octahedral cations, Clay Miner. 22 (2) (1987) 225–232.
[17] APHA, Standard Methods for the Examination of Water and Wastewater, 20th ed., APHA, AWWA, WEF, Washington, DC, 1998.
[18] J.A. Schwarz, C.T. Driscoll, A.K. Bhanot, The zero point charge of silica–alumina oxide suspensions, J. Colloid Interface Sci. 97 (1) (1984) 55–61.
[19] K.A. Krishnan, A. Sheela, T.S. Anirudhan, Kinetic and equilibrium modeling of liquid-phase adsorption of lead and lead chelates on activated carbons, J. Chem. Technol. Biotechnol. 78 (2003) 642–653.
[20] N.I. Chubar, V.F. Samanidou, V.S. Kouts, G.G. Gallios, V.A. Kanibolotsky, V.V. Strelko, I.Z. Zhuravlev, Adsorption of fluoride, chloride, bromide, and bromate ions on a novel ion exchanger, J. Colloid Interface Sci. 291 (1) (2005) 67–74.
[21] D.M. Manohar, K.A. Krishnan, T.S. Anirudhan, Removal of mercury(II) from aqueous solutions and chlor-alkali industry wastewater using 2-mercaptobenzimidazole-clay, Water Res. 36 (2002) 1609–1619.

[22] K.P. Sao, M.D. Mathew, A.R. Janana, P.K. Ray, Cellulose Chem. Technol. 21 (1985) 2–17.
[23] M.A. Khan, S.M. Ashraf, V.P. Malhotra, Development and characterization of a wood adhesive using bagasse lignin, Int. J. Adhes. Adhes. 24 (2004) 485–493.
[24] A.K. Rana, R.K. Basak, B.C. Mitra, M. Lawther, A.N. Banerjee, Studies of acetylation of jute using simplified procedure and its characterization, J. Appl. Polym. Sci. 64 (8) (1997) 1517–1523.
[25] C. Gong, D. Chen, X. Jiao, Q. Wang, Continuous hollow a-Fe_2O_3 and α-Fe fibers prepared by the sol–gel method, J. Mater. Chem. 12 (2002) 1844–1847.
[26] J.T. Keiser, C.W. Brown, R.H. Heidersbach, The electrochemical reduction of rust films on weathering surface, J. Electrochem. Soc. 129 (1982) 2686–2689.
[27] L. Li, X. Liu, Y. Ge, R. Xu, Structural studies of pillared saponite, J. Phys. Chem. 97 (1993) 10389–10393.
[28] Y.S. Ho, G.S. McKay, The kinetics of sorption of divalent metal ions onto sphagnum moss peat, Water Res. 34 (3) (2000) 735–742.
[29] N. Ozturk, T.E. Bektas, Nitrate removal from aqueous solution by adsorption onto various materials, J. Hazard. Mater. B 112 (2004) 155–162.
[30] P.B. Bhakat, A.K. Gupta, S. Ayoob, S. Kundu, Investigations on arsenic(V) removal by modified calcined bauxite, Colloid Surf. A Physicochem. Eng. Asp. 281 (2006) 237–245.
[31] S. Karaca, A. Gurses, M. Ejder, M. Acikyildiz, Kinetic modeling of liquid-phase adsorption of phosphate on dolomite, J. Colloid Interface Sci. 277 (2004) 257–263.
[32] C. Namasivayam, K. Prathap, Recycling Fe(III)/Cr(III) hydroxide, an industrial solid waste for the removal of phosphate from water, J. Hazard. Mater. B123 (2005) 127–134.
[33] R.K. Tiwari, S.K. Ghosh, D.C. Rupainwar, Y.C. Sharma, Managing aqueous solutions rich in Mn(III): an inexpensive technique, Colloids Surf. 70 (1993) 131–137.
[34] L. Zeng, X. Li, J. Liu, Adsorptive removal of phosphate from aqueous solutions using iron oxide tailings, Water Res. 38 (2004) 1318–1326.
[35] Y. Li, C. Liu, Z. Luan, X. Peng, C. Zhu, Z. Chen, Z. Zhang, J. Fan, Z. Jia, Phosphate removal from aqueous solutions using raw and activated red mud and fly ash, J. Hazard. Mater. B137 (2006) 374–383.
[36] E.W. Shin, K.G. Karthikeyan, M.A. Tshabalala, Orthophosphate sorption onto lanthanum-treated lignocellulosic sorbents, Environ. Sci. Technol. 39 (2005) 6273–6279.
[37] K.G. Karthikeyan, M.A. Tshabalala, D. Wang, M. Kalbasi, Solution chemistry effects on orthophosphate adsorption by cationized solid wood residues, Environ. Sci. Technol. 38 (2004) 904–911.